In-situ Characterisation of a Nanoparticle Jet

Robert Lindner[1], Matthias Dieckmann[1], Michael Türk[2]

1. Life and Physical Sciences Instrumentation Section TOS-MMG/ESTEC, European Space Agency, Keplerlaan 1, 2200AG Noordwijk, The Netherlands
2. Institut für Technische Thermodynamik und Kältetechnik, Universität Karlsruhe, Engler-Bunte-Ring 21, 76128 Karlsruhe, Germany

We applied Schlieren imaging and Dynamic Light Scattering (DLS) to characterize a particle gas jet, which is generated by Rapid Expansion of a Supercritical CO_2/Ibuprofen Solution through a 50µm nozzle. Schlieren images, with a field of view of approx. 10x10mm^2, revealed qualitatively density gradients of the jet, the location of the Mach disk, and the extension of the jet. Dynamic Light Scattering at a distance of about 3mm from the nozzle exit of the jet delivered a continuous decrease of count rates over the experiment duration e.g. from 180 to 2kHz and Auto-Correlation Functions (ACF) with oscillation periods spanning from 5 to 20 µs allowing for velocity estimates of some 0.06m/s perpendicular to the particle jet axis, and under these defined measurement conditions two distinct decay times around 3 and 90 µs together with intercepts ranging from some 44 to 1.1 allowing for a mean particle number concentration estimate ranging from some 0.02 to 1 particle in the scattering volume of 50 x 500µm.

1. Introduction

The production and utilization of nanoparticles is an increasing field for industrial and scientific applications, such as advanced materials, catalysts, semiconductors, optical components and precursor materials used in ceramic and pharmaceutical industry. Several new processes are promising for the production of particles, avoiding the disadvantages of classical techniques, like milling, crystallization and subsequent cleaning. The Rapid Expansion of Supercritical Solutions (RESS) process is such an environmentally compatible process [1, 2, 3]. It uses supercritical fluids (e.g. CO_2), which are characterized by densities very close to those of liquids and mass transfer properties (viscosities and diffusivities) lying between those of gases and liquids. This makes them attractive solvents for separations and reactions. The key idea behind RESS is to dissolve the solute of interest in a compressed fluid, followed by an extremely fast phase change from the supercritical to the gas-like state caused by the rapid expansion from supercritical to ambient pressure trough a nozzle. Due to the very high attainable super saturation in the free jet, particle formation occurs by homogeneous nucleation in the initial formation stage. After nucleation the particles grow either by coagulation or by condensation until super saturation disappears. However, the on-line characterisation of the jet in the transonic and supersonic

regime and the particle genesis is not completed, due to the high jet velocities and gradients in small dimensions together with variables difficult to access by measurement.

2. Experimental Set-up

2.1 The RESS Set-up

A schematically representation of the apparatus is shown in Fig. 1. This apparatus is designed for experiments in the temperature range from 270 to 370 K and pressures up to 25 MPa. Pure CO_2 is condensed from a solvent reservoir into the thermostatic extraction unit (high-pressure cell (5) with basket insert (4)) until the desired amount of solvent is charged into the cell. Heating the liquid CO_2 to the desired supercritical temperature pressurizes the system. Thereby the supercritical solvent is loaded with the solute (Ibuprofen) and thermal equilibrium is reached usually within 15 minutes. Thereafter, pure CO_2 flows through the bypass section of the extraction unit (2) and the capillary nozzle (1) to minimize the unsteadiness of the flow and to accelerate thermal equilibrium. After equilibrium, the valve (3) at the top of the high-pressure cell is carefully opened and the supercritical solution (CO_2 and Ibuprofen) flows through the thermostated duct to the capillary nozzle. By adjusting the temperature of the high pressure cell the pressure is maintained above 18-20 MPa for about 10-15 minutes. Figure 2 shows the dimensions of the expansion nozzle.

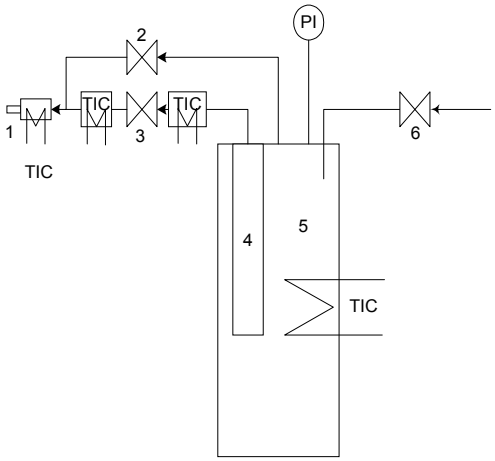

Fig. 1: The mobile RESS batch reactor

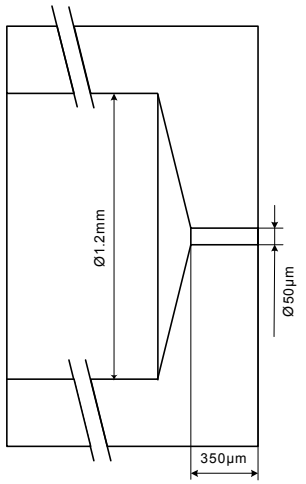

Fig. 2: Schematic drawing of the expansion nozzle 1

2.2 Schlieren Imaging

Schlieren Images visualise jet morphologies in terms of density gradients and DLS facilitates preliminary approaches to derive jet velocities and viscoelastic system properties.
Schlieren and shadowgraph imaging are old established techniques for flow visualisation and are often used for qualitative measurements of refractive index and hence density gradients. Schlieren technology utilizes a light source, an imaging lens and an image plane to capture “bent” light paths due to light refraction. Light refraction is caused by a change in the refractive

index of the fluid at different temperatures and densities. The result is a well-defined image illustrating the fluid at different densities and temperatures [4].

2.3 Dynamic Light Scattering

DLS is a velocity measurement, in case of particle sizing, of mere Brownian motion corresponding to the characteristics of registered scattered light intensity fluctuation [5]. The self-similarity of the recorded intensity fluctuations is calculated. The achieved ACF can be described as an exponential decay $g_2(t)$, whereas 1 indicates the baseline to which the ACF decays and β equals the ordinate position intercepted by the ACF, often referred to as the Intercept.

$$g_2(t)=1+\beta e^{-\Gamma t} \tag{1}$$

This classical formula is valid only for a Gaussian distribution of spherical scattering centers having no number fluctuation within the scattering volume.
The characteristic decay time is given by

$$\tau_1=\frac{1}{\Gamma}=\left(2q^2 D_{St}\right)^{-1} \tag{2}$$

$$\text{with } |q|=\frac{4\pi n}{\lambda}\sin\left(\frac{\theta}{2}\right) \tag{3}$$

and D_{st} = diffusion coefficient, q = scattering vector, with the refractive index n, the illumination wavelength λ and the scattering angle θ. This links under ideal conditions directly to the hydrodynamic radius, r_p of the stray light center by the Stokes-Einstein equation:

$$D_{St}=\frac{k_B T C u}{6\pi\eta r_p} \tag{4}$$

The Stokes Einstein equation is extended by the Cunningham factor Cu, accounting for the slip between gas phase and particles [6], with k_B Boltzmann constant, T Temperature, η dynamic viscosity and r_p the hydrodynamic particle radius.
The inverse value of the intercept equals to the mean scattering centre number in the scattering volume [7].
The ACF is evaluated by a non-linear fit program abbreviated CONTIN [8] yielding decay time distributions to be converted into radii.
DLS is a state-of the art technique to characterise liquid particle systems in the size range of a few nm to µm , but applications to aerosols are still rare. Hind and Reist were the first who investigated quasistatic aerosols [9]. Further applications were focused on soot analysis in combustion processes. Weber and Schweiger applied successfully DLS to a quasi monodisperse laminar flowing aerosol, retrieving particle size, particle number concentration and flow velocity [10]. However, measurements on turbulent and transonic systems have not yet been performed.
In case of monodisperse aerosols flowing into one direction, a theoretical model of the normalised autocorrelation function can be fitted to the measured data [10]. The below equation represents an extension of the equation (1):

$$g_2(t)=\left[1+\beta e^{\left(-\frac{t}{\tau_1}\right)} e^{\left(-\frac{t^2}{\tau_{21}^2}\right)}+\frac{e^{\left(-\frac{t^2}{\tau_2^2}\right)} 2^{-1.5}}{N}\right] \tag{5}$$

where

$$\tau_2 = \frac{w_0}{v_x} \tag{6}$$

with w_0 as the beam waist radius of the scattering volume and vx the velocity in the scattering volume. Due to the uncertainties regarding the overlap of transmitting and receiving beam together with additional alignment inaccuracies of this optical assembly towards their matching to the aerosol jet, normalisation constants such as 2-1.5 in equation (5) are only valid as rough approximations. N is the particle number in the scattering volume and f the contrast factor, set to one for a monomodal acquisition.

We used a DLS-system, developed by Dierks and Partner in its main characteristics comparable with the one described in [11] and [12]. The main DLS system characteristics are briefly given here: One solid state laser with 30mW, lasing at 689.5nm is temperature controlled at room temperature with an accuracy of approx. ±0.05ºC and illuminates via optical coupler (loss approx. 50% under field conditions) and a mono-mode optical fiber a scattering volume spanned by receiver and transmitter collimators to yield a 50x500µm sized scattering volume for backscattering configuration at an angle of 155º. A second NdYAG laser with an output power of 30mW, lasing at 532.8nm is delivered to the scattering volume by focused optics with a focal length of f=60mm at a scattering angle of 90º. The mono-mode receiver is fed for both used illuminations into Photo-Multiplier Tubes (PMT) with a quantum efficiency of approx. 5% at 689.5nm, and some 15% for 532.8nm. The PMT's deliver via pulse shaper the signals to a real-time correlator with a first sampling time starting at 800ns and a sampling time structure spanning 10 decades. The optical fibers connect by fiber connectors the DLS system with dedicated various optical mounts implemented close to the aerosol jet. As various mono-mode optrodes were used a super positioning of the green and red laser facilitated alignment verification. The optrode is a transmitter/receiver-combined backscattering configuration. A computer system accomplishes all operations such as laser temperature stabilisation, data evaluation and selection of measurement times, which is varied between 20s and 200s for the data presented here. In Figure 3 the DLS optrode arrangement in combination with the RESS jet is represented schematically.

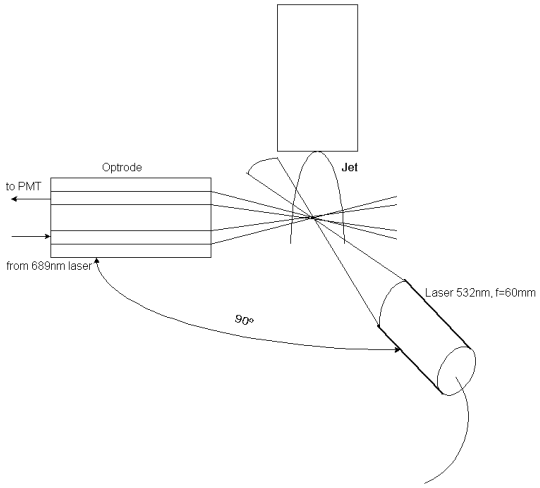

Fig. 3 Schematic of the DLS set-up for measurement in the Aerosol jet

The DLS system is a development achieved within the frame of the basic Technology Research Program of the European Space Agency and produced results in various research areas [13].

3. Results

Schlieren pictures were taken with a combined Schlieren and Mach-Zehnder Interferometer set-up, whereas only the Schlieren function was used.
Figure 4 shows a picture of the jet, consisting of pure CO_2. The Mach Disk is visible in a distance of about 0.46mm from the nozzle outlet. This values is well in line with the correlation

$$L = 0.67D\sqrt{\frac{p_0}{p_1}} \tag{7}$$

from Askhenas and Sherman [14], where L is the distance of the Mach Disk, D the nozzle diameter (50µm) and p_0 and p_1 are the initial pre-expansion pressure (18-20MPa) and the background pressure (0.1MPa).

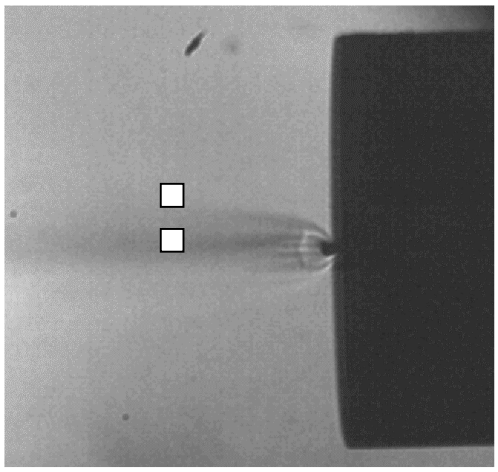

Fig. 4 Schlieren image of a pure CO_2 jet without particle production, the cylinder containing the nozzle (black) has a diameter of 6.4mm, the distance to the first visible shock wave is approx. 0.45mm. The white squares show the approximate location of the DLS measurements

Several Measurements were performed with the DLS set-up. As shown in Figure 5, the count rate decreased continuously from due to a decrease in particle concentration as a consequence of the pressure drop in the extractor. Many parameters necessary for a precise determination of particle sizes from the ACF, such as temperature, pressure, viscosity and refractive index in the scattering volume are not accessible yet. Hence it was intended to see, whether a meaningful ACF can be retrieved at all from a highly diluted and highly turbulent system like this nanoparticle jet.
Count rates without a jet ranged between 100-400Hz. Count rates with a pure CO_2 jet (extractor empty) were registered in the area of about 0.5-1.2kHz and with an aerosol/gas jet between 2-180kHz.

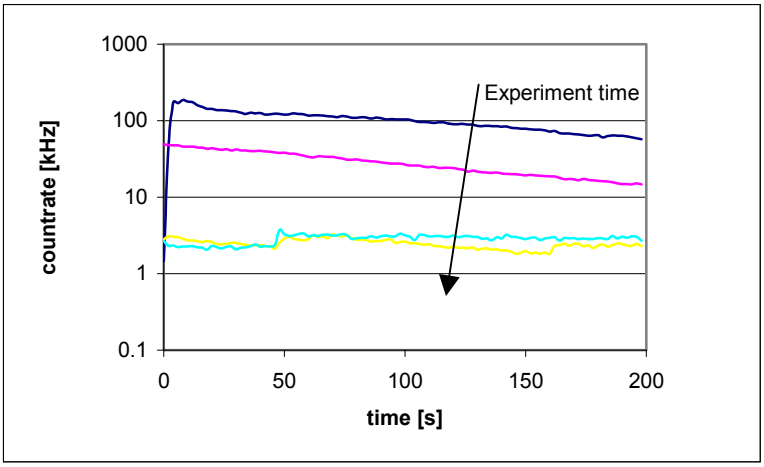

Fig. 5 Typical count rate decreases of consecutive measurements during an experiment within 15 minutes. Highest count rates were registered shortly after opening of valve (3) as shown in Fig. 1

Figure 6 shows ACF of typical measurements as beta values versus time. Two types of acf have been observed, those with high beta values ranging from 44 to 4 (6a) and those with beta values below 2 (6b).

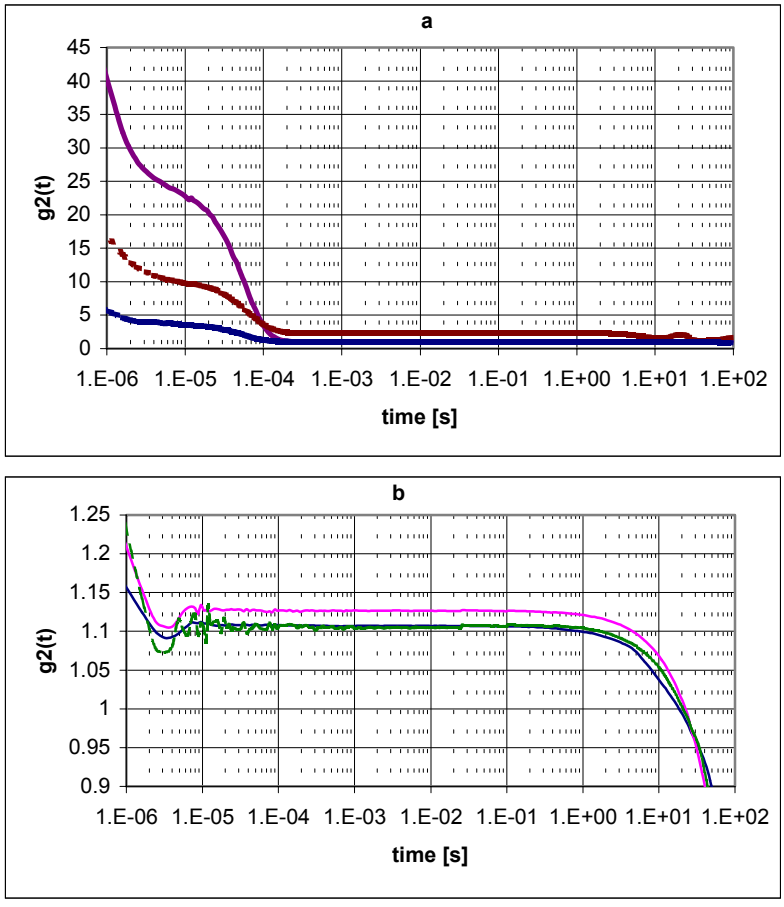

Fig. 6a+b Autocorrelation functions measured in the outer area (a) and in the central area (b) of a CO_2/particle jet

In 6a, two different decay times are clearly visible at about 3 µs and 90 µs. These correspond to the factors τ_2 and τ_1 in equation 4. A value for τ_2 of 3 µs would correspond to a particle speed of 16.7 m/s confirming that the measurement is in the subsonic area of the particle jet. This can be deduced from equation 4, because only if the flow velocity is lower than the diffusion velocity, τ_2 is longer than τ_1 so that the term with the two multiplied exponentials does not vanish. The measured time constant 90µs (τ_1) is compatible with a Brownian motion of particles with an approx. diameter of 500nm in CO_2. The intercept, i.e. the extrapolated interception between ordinate at t = 0 and measured ACF, is a measure for the number concentration in the scattering volume ranging here from 44 to 6, revealing particle number concentrations from 0.02 to 0.2 in the scattering volume (the intercept is inverse proportional to the particle number concentration). The interested reader may consult [14] for the detailed considerations of the theory of DLS. These measurements have been performed in the peripheral range of the jet.
Fig. 6b shows three ACF with a low intercept from measurements closer to the jet centre. In the centre of the jet, the velocity is much higher, thus the diffusion cannot be measured anymore ($\tau_2 < \tau_1$). Clearly visible are oscillations between 5 and 20µs, which are a Doppler shift of the scattered light, due to a directed movement of the particles in the jet in observation direction. With the associated Doppler frequency, the velocity v equals to

$$v = \frac{c}{n}\frac{\Delta f}{f} \tag{7}$$

Where Δf corresponds to 1/oscillation period and f equals the frequency of the used laser light (563.9THz for 532nm) and n is the refractive index, assumed to be 1.1. With a typical oscillation period of about 8µs, a velocity of approx.0.06m/s results. One has to bear in mind that this velocity normal to the face of the detector caused by the particle jet expansion is difficult to separate from slight misalignments between the jet and the field of view of the receiver, which may cause similar oscillations. Consequently, this approach presents a first estimate. The roll off of $g_2(t)$ between 1s and 100s in Figure 6b coincides with a decrease of count rate during the measurement, as shown in Figure 5.

4. Conclusions

DLS measurements in a nanoparticle jet are possible. Depending on the measurement location, different types of ACF were retrieved in a reproducible way, which need to be studied further with regard to their physical meaning. Different decay times and oscillations in the ACF were observed. Decay times measured in the outer region of the particle jet can roughly be linked to a particle diameter (τ_1) of, say, approx. 500nm possibly indicating a ripening or second generation particle formation region, and an axial velocity component (τ_2) of approx. 16.7m/s. Oscillations in the ACF measured in the centre of the jet reveals a velocity component normal to the face of the detector of approx. 0.06m/s, with the reservations indicated above. The intercept variation reveals number concentrations of 0.02-1 particles in the scattering volume of 50x500µm. Schlieren imaging yields the dimensions of the jet and confirmed the position of the Mach Disk at about 0.46mm.

5. Acknowledgments

The authors wish to thank Dr. L. Joannes and Mr. S. Farinotti from Lambda-X for providing us with the possibility to perform the Schlieren measurements. Thanks are also due to Dr. K. Dierks for his support concerning the DLS evaluation.

6. References

[1] Tom, J. W., Debenedetti, P. G.; Particle Formation with Supercritical Fluids - A Review; *J. Aerosol Sci*. **22** (1991), 555-584

[2] Türk, M., Formation of small organic particles by RESS: Experimental and Theoretical Investigations, *J. Supercrit. Fluids* (1999) **15**: 79-89

[3] Türk, M.: Influence of thermodynamic behaviour and solute properties on homogeneous nucleation in supercritical fluids, *J. Supercrit. Fluids*, (2000) **18**, 3, 169-184

[4] Settles, G.S., Schlieren and Shadowgraph Techniques: Visualizing Phenomena in Transparent Media, *Springer-Verlag*, Nov. 2001

[5] Cummins, H. Z., Pike, E.R., "Photon Correlation spectroscopy and velocimetry" *Plenum Press New York*, 1977

[6] Hutchins, D.K., Harper, M.H., and Felder, R.L., *Aerosol Sci. Technol*. **22**, 202 (1995)

[7] Rička, J., Fluctuations and Correlations: Dynamic Light Scattering, *Habilitation,* Bern, Jan.1994

[8] Provencher, S. W., "CONTIN: A general purpose constrained regularization program for inverting noisy non-linear algebraic and integral equations", *Computer Phys. Comm.* **27**, p.229-242 (1982)

[9] Hinds, W., Reist, P.C., *Aerosol Sci*., **3**, 501 (1972)

[10] Weber, R., Schweiger, G. *Colloid and Interface Science*, **210**, 86-96 (1999)

[11] H. Auweter, D. Horn, "Fibre-Optical Quasi-elastic Light Scattering of concentrated Dispersions" *Colloid and Interface Science*, Vol. **105**, pp. 399-409, No. 2, June 1985.

[12] Dierks K., Dierks & Partner, "Product description of DLS systems", 1994

[13] Dieckmann, M. W. M., Dierks, K., Characterisation of selected bio-molecules in the course of the STS-95 mission, using diagnostics developed within ESA's Technology and Research Program, Conference on Material and Nanotechnologies, Instrumentation for material synthesis and near field optical microscopy, *SPIE Proceedings* **Vol. 4098**, p.11-25, 2000

[14] Askhenas, H., Sherman, F.S. Rarefied Gas Dynamic. **Suppl. III, Vol. II**: 4th International Symposium; de Leeuw, J.H., Ed.; *Academic: New York*, 1966; pp84-105